OPEN ACCESS

University of BRISTOL

Link to published version (if available):
10.1016/j.physleta.2006.03.003

Link to publication record in Explore Bristol Research
PDF-document

On the genesis of spike-wave oscillations in a mean-field model of human thalamic and corticothalamic dynamics

Serafim Rodrigues*, John R. Terry* and Michael Breakspear+

(*) Department of Mathematical Sciences, Loughborough University, Leicestershire, LE11 3TU, UK

(+) Black Dog Institute, Randwick, NSW, 2031, Australia and
School of Psychiatry, UNSW, NSW, 2030, Australia

November 8, 2005

Abstract

In this letter, the genesis of spike-wave activity - a hallmark of many generalized epileptic seizures - is investigated in a reduced mean-field model of human neural activity. Drawing upon brain modelling and dynamical systems theory, we demonstrate that the thalamic circuitry of the system is crucial for the generation of these abnormal rhythms, observing that the combination of inhibition from reticular nuclei and excitation from the external signal, interplay to generate the spike-wave oscillation. The mechanism revealed provides an explanation of why approaches based on linear stability and Heaviside approximations to the activation function have failed to explain the phenomena of spike-wave behaviour in mean-field models. A mathematical understanding of this transition is a crucial step towards relating spiking network models and mean-field approaches to human brain modelling.

1   Introduction

Epilepsy is a relatively common neurological disorder, with a life-time prevalence of approximately 1%. The generalized seizures (tonic-clonic and Absence) are defined as those associated with abnormal activity across most, or all, of the cortex. Several models have been proposed to explain the aggregated electrical activity of large scale neuronal populations, or mass action brain models. Pioneering work in this area was performed by Wilson and Cowan [1], which was generalized to account for functional activity within the brain by Nunez [2] and Freeman [3]. During the last decade, several groups have advanced mass-action neural models to incorporate a range of increasingly plausible neurophysiological

1

processes [4, 5]. Robinson and co-workers explicitly incorporated thalamic circuitry and analytically described the propagation and stability of electrical activity within the cortex by means of a damped wave equation [6].

Absence seizures occur predominantly in children and are characterized by brief, intermittent interruptions to consciousness. Preliminary studies of seizures generated by the model [7] have demonstrated that it can correctly predict the occurrence of spike-wave morphologies (~3Hz paroxysmal oscillations) which are the hallmark of Absence seizures. In this mean-field model, the two main subdivisions of the thalamus, the reticular nuclei and the specific relay nuclei, are both implicated in the generation of seizure waveforms. Other studies have indicated a crucial role of the specific relay nuclei underlying the generation of oscillations. In particular, it is widely accepted (both, through in-vitro and in-vivo experiments, and modelling) to play a pivotal role in the generation of spike-wave activity [8, 9, 10, 11].

Computational models of cortical and corticothalamic circuits have been increasingly employed to explain a variety of healthy and pathological states [12]. However, the vast majority of such studies rely exclusively upon either numerical integrations or analytic treatment of linear approximations. The analytic treatment of nonlinear phenomena is in contrast, underdeveloped. A major objective of the current paper is to address this problem via a thorough mathematical analysis of the onset of Absence seizures, which is of both clinical and computational significance. The consequent simplifications of the full system to make it mathematically tractable can be justified by noting that purely numerical studies of high dimensional system of delay differential equations are vulnerable to systemic errors from a variety of sources.

The model we consider [6] provides a unified description of both the EEG (Electroencephlogram) recorded at rest and the ERPs (Evoked Response Potentials) which occur following a sensory input. It incorporates a wide-range of neurophysiological processes, including excitatory and inhibitory neural populations, axonal and dendritic time lags, long range excitation, and the low-pass filter effect of dendritic integration on incoming impulses. Importantly, the model incorporates the main features of corticothalamic loop which are believed to be one of the mechanisms for epileptogenesis [10]. These include excitatory inputs between the cortex and the specific relay nuclei, the excitatory influence of the cortex and the specific relay nuclei on the reticular nuclei, and the inhibitory feedback from the reticular nuclei onto the specific relay nuclei. An important consideration is that this mean-field description does not explicitly consider ionic currents, which are believed to play a crucial role in the generation of many common EEG rhythms. For example, the work of Sejnowski and Destexhe [10, 11] has implicated $GABA_B$ in evoking spike-wave oscillations in network models based on interactions at the microscopic level. In the approach considered here, such currents have been averaged out and fitted parametrically from data. Hence these currents are incorporated implicitly in the model. The relationship between microscopic and macroscopic approaches to brain modelling is currently an open question in the field and consequently, understanding mathematically how a mean-field model can produce oscillations resembling spike-wave

activity, is crucial as a step towards relating these two approaches.

2   Description of the model

By definition, generalized seizures are characterised by the appearance of abnormal seizure activity almost simultaneously in all cortical or scalp EEG channels such that the defining features (i.e. spike-wave etc.) appear globally [11]. This suggests that the underlying dynamics may reflect very large-scale or even global brain processes and motivates the reduction of the evolution equations from a system of delayed Partial Differential Equations to a system of delayed Ordinary Differential Equations. Further, only the thalamic circuitry driven by an external signal is considered. There are several motivating factors for this consideration. Firstly, in clinical EEG recordings of the onset of absence seizures, the transition from pre-ictal to ictal dynamics is typically heralded by oscillatory behaviour, prior to spike-wave activity being observed, as illustrated in Figure 1. This feature was also observed in our preliminary study of the full model [7], where we observed that in the absence of a cortical signal, the thalamic subsystem was quiescent and that spike-wave activity (a periodic signal with an extra spike per period) was generated via periodic dynamics from the cortex fed into both specific relay nuclei and the reticular nuclei populations. The strength of modulation of this signal into the specific population was observed to be the crucial parameter for generation of such rhythms (see also Figure 1). Further observations from the full model suggest that there is a phase shift in the dynamics of the *specific* neuronal populations when compared to both *cortical* and *reticular* populations. This feature is supported by both *in-vivo* and *in-vitro* experiments [8, 9, 10, 11] which demonstrate that spike-wave activity is first initiated in the specific relay nuclei, which then propagates to the cortex and is finally induced in the reticular nuclei.

Thus, as an approximation to the full model after the first nonlinear bifurcation has occurred, we consider only the thalamic circuitry driven by an external periodic signal. This reduced model is defined by

$$\begin{cases} \frac{1}{\alpha\beta}\left[\frac{d^2}{dt^2}V_r(t) + (\alpha+\beta)\frac{d}{dt}V_r(t) + \alpha\beta V_r(t)\right] = \nu_{rs}\sum[V_s(t)] + \nu_{re}\phi_{\text{external}}, \\ \frac{1}{\alpha\beta}\left[\frac{d^2}{dt^2}V_s(t) + (\alpha+\beta)\frac{d}{dt}V_s(t) + \alpha\beta V_s(t)\right] = \nu_{sr}\sum[V_r(t)] + \nu_{se}\phi_{\text{external}} + \nu_{sn}\phi_n. \end{cases} \tag{1}$$

where

$$\sum[V_a(t)] = \frac{Q_a^{\text{max}}}{1 + \exp\left(-\frac{\pi}{\sqrt{(3)}}\frac{V_a(t)-\theta_a}{\sigma_a}\right)}$$

is a unipolar sigmoidal function representing the relationship between the transmembrane potential V_a and the axonal firing rate. Descriptions and typical values of these parameters are provided in Table 1. System (1) models the averaged postsynaptic activity at the cell soma. It relates the induced transmembrane voltage $V_a(t)$ with the incoming pulses $\phi_a(t)$ where $a = \{r, s\}$ (reticular nuclei and specific relay nuclei). The perturbation in the induced transmembrane voltage propagates along dendrites and reaches the cell body with some attenuation and lag. Thus, α and β are constants representing the inverse rise and decay times parameterising the dendritic response to these impulses.

This model is illustrated schematically in Figure 2. A similar model for the study of olfaction has been considered in [13] where linear stability analysis was performed and stability curves in the parameters space were derived.

3   Analysis of the periodically forced model

As mentioned previously, in-vivo and in-vitro experiments from animal models [11], as well as our own extensive numerical simulations of both the full and reduced models suggest that the abnormal rhythms associated with Absence seizures initially appear in the specific relay nuclei. Subsequently, if the excitation between specific to reticular, or specific to cortex, is strong enough then these abnormal rhythms may also be observed there. Simulations (see Figure 3) also indicate that the subthalamic input plays no part in the generation of abnormal rhythms. We further observe that the solutions to $V_r(t)$ are always periodic and that only the amplitude of these oscillations change when the parameters are varied.

Thus, for the purposes of understanding the genesis of abnormal activity in this reduced case, we make the following assumptions. First, we assume that there is no interactions between the specific relay nuclei and the reticular nuclei populations, i.e. $\nu_{rs} = 0$. Second, we assume that the subthalamic input is also zero, i.e. $\nu_{sn} = 0$.

Under these assumptions, the homogeneous solution for the individual modules is a combination of decaying exponentials. This can be seen by studying the roots of the characteristic polynomial derived from either of the differential operators in (1),

$$r^2 + (\alpha + \beta)r + \alpha\beta = 0,$$

the solution for which is given by

$$V_a^h(t) = Ae^{(-\alpha t)} + Be^{(-\beta t)}. \tag{2}$$

A further important point to note is that the dynamics of each individual system is overdamped; with the damping factor given by $\zeta = \frac{(\alpha+\beta)}{2\sqrt{(\alpha\beta)}} > 1$. This demonstrates that spike-wave activity can not occur due to any intrinsic dynamics within the individual thalamic modules.

3.1   Forcing function $\phi_{external} = \sin(\omega t)$

For the purposes of analysing the model, we consider a particular form of the forcing function, $\phi_{external} = \sin(\omega t)$. In the absence of the excitatory input from the specific relay nuclei, the solution for the reticular nuclei can then be derived explicitly and is given by:

$$V_r^p(t) = K\sin(\omega t + \delta) \tag{3}$$

where $K_a = \sqrt{(C_a^2 + D_a^2)}$ and $\delta_a = \arcsin(D_a/K_a)$ with

$$C_a = \frac{(\alpha\beta - \omega^2)\nu_{re}\alpha\beta}{((\alpha + \beta)^2\omega^2 + (\alpha\beta - \omega^2)^2)(\alpha\beta - \omega^2)}$$

and

$$D_a = -\frac{\omega\nu_{ae}\alpha\beta(\alpha + \beta)}{(\alpha + \beta)^2\omega^2 + (\alpha\beta - \omega^2)^2}$$

Note that this particular solution is also valid for the external forcing part of the specific module, i.e. $a = \{r, s\}$.

Consequently the long-time behavior of the specific module, $V_s(t)$, is governed by the solution of the differential equation:

$$\frac{1}{\alpha\beta}\left[\frac{d^2}{dt^2}V_s(t) + (\alpha + \beta)\frac{d}{dt}V_s(t) + \alpha\beta V_s(t)\right] = \nu_{sr}\sum[V_r(t)] + \nu_{se}\phi_{external} \tag{4}$$

where $V_r(t)$ is given in equations (2) and (3).

Since Σ is a unipolar sigmoidal function, the resulting equation is transcendental and consequently an explicit solution to this equation is not possible. However, a result from [14] shows that it is possible to relate the stability of the full system to that of a related piecewise linearized system. Essentially, we perform a piecewise linearization of the unforced system and then reapply the forcing term in each case. In order to do this, we obtain steady-states for $V_r^\star$ and $V_s^\star$ of the system, using the numerical software package XPP [15]. Linearizing about these steady-state gives the following:

$$\frac{dx}{dt} = \mathbf{L}x + \mathbf{B}u, \tag{5}$$

where the vector $\mathbf{B}$ comes from the external drive,

$$\mathbf{B} = \begin{pmatrix} 0 \\ \alpha\beta\nu_{se}\sin(\omega t) \\ 0 \\ \alpha\beta\nu_{re}\sin(\omega t) \end{pmatrix},$$

and $\mathbf{L}$ is the piecewise linear vector field of the system,

$$\mathbf{L} = \begin{pmatrix} 0 & 1 & 0 & 0 \\ -\alpha\beta & -(\alpha + \beta) & \alpha\beta\nu_{sr}y_\sigma(V_r^\star) & 0 \\ 0 & 0 & 0 & 1 \\ \alpha\beta\nu_{rs}y_\sigma(V_s^\star) & 0 & -\alpha\beta & -(\alpha + \beta) \end{pmatrix}.$$

Essentially $\mathbf{L}$ is the Jacobian matrix of the unforced system for each of the piecewise linear segments of the function Σ. The first order Taylor approximation of this function at a point x_0, is given by

$$y(v)|_{x_0} = \frac{Q^{max}}{1 + e^{-\frac{\pi}{\sqrt{3}}(\frac{x_0 - \theta}{\sigma})}} + (v - x0)\frac{\frac{Q^{max}\pi}{\sigma\sqrt{3}}e^{(-\frac{\pi}{\sqrt{3}}(\frac{x_0 - \theta}{\sigma}))}}{[1 + e^{(-\frac{\pi}{\sqrt{3}}(\frac{x_0 - \theta}{\sigma}))}]^2} + H.O.T. \tag{6}$$

Hence, the specific piecewise approximation we consider is

$$
y_\sigma(v) = \begin{cases} y(v)|_{V_s^*} & -\infty \le v < b, \\ y(v)|_{V_r^*} & b \le v < \infty, \end{cases} \tag{7}
$$

where $b > 0$ is the intersection point of the lines (at this point the derivative loses continuity). Note that we could have considered more line segments in the whole domain of the function Σ. However, this would not change the conclusions, as the solution $V_r(t)$ is bounded and evolves around a steady state and consequently the solution for $V_s(t)$ will also be bounded. Considering more approximations will only smooth out the solutions obtained.

The composition of this piecewise linear approximation $y_\sigma(v)$ in (7) with the explicit solution for $V_r(t)$ given in (3) results in two regions of interest:

$$
\text{Region}_\text{I} = \left\{ t \in \mathbb{R}, N \in \mathbb{Z} : \frac{\arcsin(\frac{b}{K}) - \delta + 2N\pi}{\omega} \le t \le \frac{\pi - \arcsin(\frac{b}{K}) - \delta + 2N\pi}{\omega} \right\}
$$

$$
\text{Region}_\text{II} = \left\{ t \in \mathbb{R}, N \in \mathbb{Z} : \frac{-\arcsin(\frac{b}{K}) - \pi - \delta + 2N\pi}{\omega} < t < \frac{\arcsin(\frac{b}{K}) - \delta + 2N\pi}{\omega} \right\}
$$

It is now possible to explicitly solve this piecewise linear appoximation to (4) using the method of variation of parameters, taking care to ensure that the boundary conditions for each interval are satisfied. The resulting asymptotic solution for $V_s(t)$ has the following form

$$
V_s(t) = \begin{cases} K_s \sin(\omega t + \delta) + \mathcal{A} V_{s*}^m \sin\left(\omega t + \widehat{\delta}\right) + f(e^{-Kt}, c), & t \text{ in Region}_\text{I}, \\ K_s \sin(\omega t + \delta) + \mathcal{B} V_{r*}^m \sin\left(\omega t + \widehat{\delta}\right) + g(e^{-Kt}, c), & t \text{ in Region}_\text{II}, \end{cases} \tag{8}
$$

where V_{r*}^m and V_{s*}^m are the amplitudes of the piecewise linear approximation to the steady state of V_r and V_s respectively. The parameters $\mathcal{A}$ and $\mathcal{B}$ incorporate the inhibitory effect of the reticular on the specific ν_{sr}, as well as α and β. There is also a different phaseshift $\widehat{\delta}$ of the composite function compared to the external forcing. The functions f and g involve exponentially decaying and constant terms, which do not effect the asymptotic form of the solution.

3.2 Description of the spike-wave solution

These key aspects of the solution (8) are illustrated in Figure 4. Essentially, the spike-wave oscillation arises as a result of the interaction of the sinusoid due to the excitatory external input and the opposite facing sinusoid-like function resulting from the composition of the piecewise linear approximation to Σ with $V_r(t)$. This composite function has the same total period as the external signal, however, it consists of two sinusoids of different amplitudes and phases acting on each of the Regions I and II. The peaks of each bump in the combined solution correspond to the transition between regions. Noting

that the area of Region$_I$ is less than that of Region$_{II}$, this can technically be classed as a spike-wave oscillation, since the area of the spike part of the solution is less than that of the wave. A comparison between the explicit solution and that numerically generated for the same case using XPP is given in Figure 5.

The fact that the solution of the two parts are opposite facing in each region is also crucial for the generation of the abnormal rhythm. Were both to point the same way, then only a one-bump solution would be observed. These opposite facing solutions are due to the inhibitory effect of the reticular nuclei on the specific relay nuclei and explains why no such solutions are ever observed in the reticular nuclei in the absence of activity in the specific relay, since the synaptic interactions between them are excitatory in nature. Finally, note that the gradient of the sigmoidal function Σ varies dramatically between the two regions and it is this marked difference in gradient that leads to the different amplitudes on each Region, which in turn gives the spike-wave solution. This illustrates the need for at least a piecewise linear approximation to Σ and explains why previous attempts using linear stability analysis and Heaviside approximations to explain this phenomena were unsuccessful.

A final point concerns time-delays in the system. The mechanisms responsible for generation of the abnormal rhythms elucidated in this letter do not require any time-delays, which is consistent with the work of [11]. However, the full model [6], from which this reduced model was obtained, has delays between cortex and thalamus. Thus, it is imperative to determine the precise role that these time-delays play in the full system. This work is currently underway.

4   Summary

In summary we have explicitly studied the mechanisms underlying the generation of a two-bump waveform within the thalamic circuitry component of a mean-field model approximating the dynamics observed in clinical human EEG. In particular, by considering a piecewise linear approximation to the sigmoidal activation function, we have been able to write down a mathematical solution explaining the transition from oscillatory to spike-wave like dynamics, demonstrating that the phenomena is due to properties of the thalamic pathways, rather than intrinsic properties of the individual thalamic modules. The spike-wave activity arises first in the specific population as a combination of excitation from the external source and inhibition from the reticular nuclei. This finding demonstrates why spike-wave behaviour is not observed first in the cortex or reticular nuclei in this mean-field model, where only excitatory processes occur. Through feedback from the thalamus to the cortex (in the full system), such a two-bump solution would, given suitable conditions, be expected to iteratively reshape cortical output. In fact, this may explain why full spike-wave activity can only be maintained in the presence of cortical excitation [11]. Such a process of iterative reshaping would be expected to have a strong influence on the eventual spike-wave character of the observed Absence seizure waveform [7].

Future work will focus on characterising the occurrence of the limit-cycle in both the reduced model and the full corticothalamic system, determining the contribution of time-delays to the dynamics of the full system and relating these macroscopic approaches to physiologically based microscopic models.

5 Acknowledgments

References

[1] H. R. Wilson and J. D. Cowan, Kybernetik **13**, 55 (1972).

[2] P. L. Nunez, IEEE Trans. Biomed. Eng. **21**, 473 (1974).

[3] W. J. Freeman *Mass Action In The Nervous System* (Academic Press, New York) (1975).

[4] J. J. Wright and D. T. J. Liley, Behav. Brain Sci. **19**, 285 (1996).

[5] V. K. Jirsa and H. Haken, Phys. Rev. Lett. **77**, 960 (1996).

[6] P. A. Robinson, C. J. Rennie and J. J. Wright, Phys. Rev. E **56**, 826 (1997); P. A. Robinson, C. J. Rennie, J. J. Wright and P. D. Bourke, Phys. Rev. E **58**, 3557 (1998); C. J. Rennie, P. A. Robinson and J. J. Wright, Phys. Rev. E **59**, 3320 (1999); C. J. Rennie, P. A. Robinson and J. J. Wright, J. Theor. Biol. **205**, 17 (2000); P. A. Robinson, C. J. Rennie and D. L. Rowe, Phys. Rev. E **65**, 041924 (2002); P. A. Robinson, C. J. Rennie, D. L. Rowe and S. C. O'Connor, Human Brain Mapping **23** 53 (2004).

[7] M. Breakspear, J. A. Roberts, S. Rodrigues, J. R. Terry and P. A. Robinson, Cereb. Cortex (in press) (2005). (A preprint is available from

`http://www.lboro.ac.uk/departments/ma/research/preprints/papers05/05-28.pdf`)

[8] G. Avazani M. de Curtis, F. Panzica and R. Spreafico, J. Physiol. **416**, 111 (1989).

[9] A. Destexhe, D. A. Contreras and T. J. Sejnowski, Biophys. J. **65**, 2474 (1993).

[10] A. Destexhe, D. A. Contreras and M. Steriade, J. Neurophys. **79**, 999 (1998).

[11] A. Destexhe and T. J. Sejnowski *Thalamocortical Assemblies* (OUP) (2001); A. Destexhe and T. J. Sejnowski, Physiol. Rev. **83**, 1401 (2003).

[12] A. Destexhe and E. Marder, Nature **431**, 789 (2004).

[13] Dongming Xu and J. C. Principe, IEEE Trans. Neural Net. **15** 1053 (2004)

[14] D. W. Jordan and P. Smith *Nonlinear Ordinary Differential Equations* (OUP) (1999).

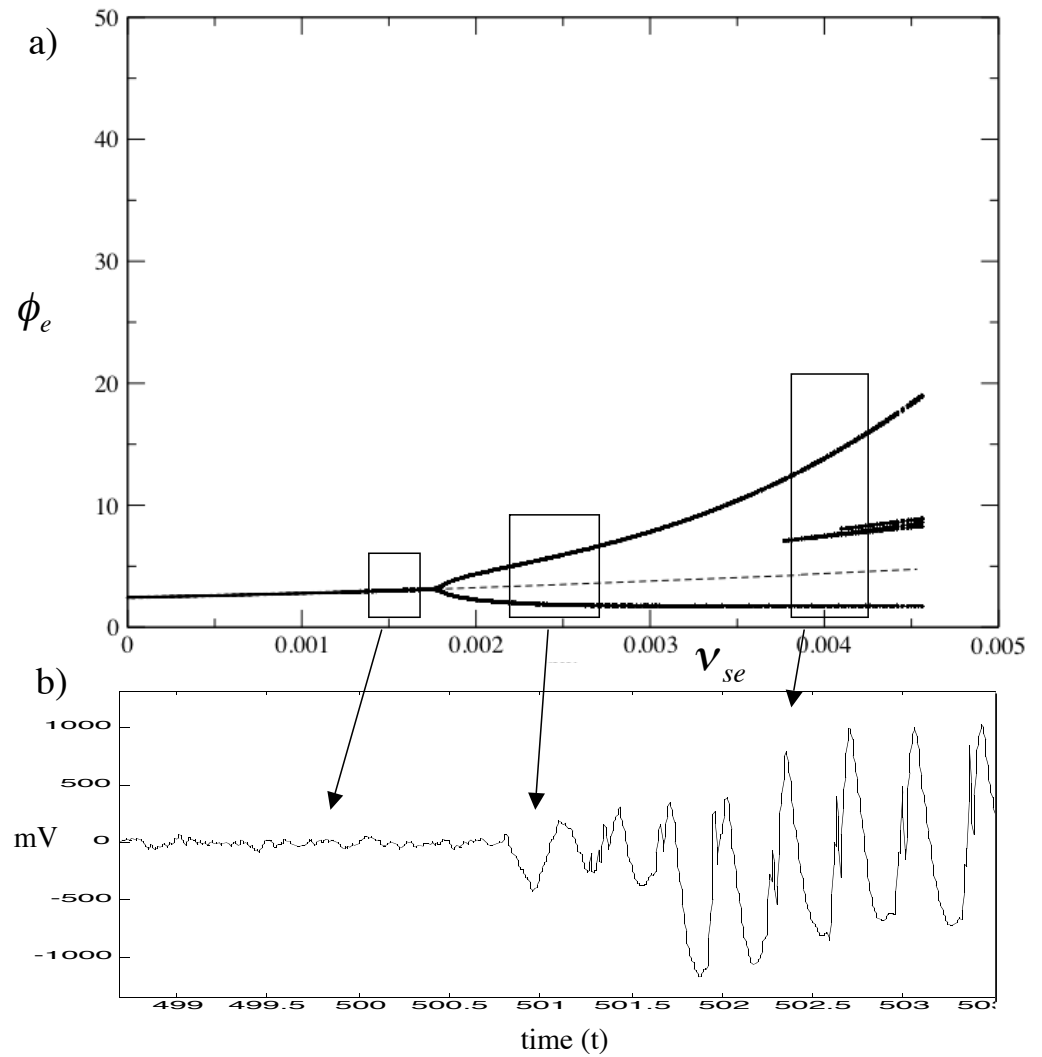[15] B. Ermentrout *Simulating, Analyzing, and Animating Dynamical Systems. A Guide to XPPAUT* SIAM (2002).

Figure 1: Illustrating a comparison between the bifurcation diagram for the full model considered in [7] (panel a)) and a clinical EEG recording during the onset of an absence seizure (panel b)). Upon varying the parameter ν_{se} there is a transition from steady-state to oscillatory dynamics, via a Hopf bifurcation, before a further transition gives rise to spike-wave like behaviour. These sequence of events replicates that observed in the clinical recording. The aim of the present letter is to characterise the transition between stage 2 (oscillatory behaviour) and stage 3 (spike-wave). Consequently, we assume the cortex is generating a periodic oscillation and thus we drive the thalamic subsystem with a periodic signal of a type that is amenable to analysis.
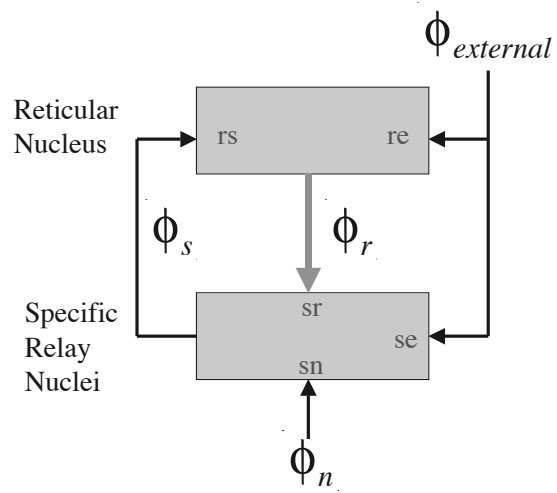
10

Figure 2: Schematic of the reduced Thalamic model considered. All interactions illustrated by thin arrows are assumed to be excitatory. The one between reticular and specific illustrated by the thick arrow is inhibitory.
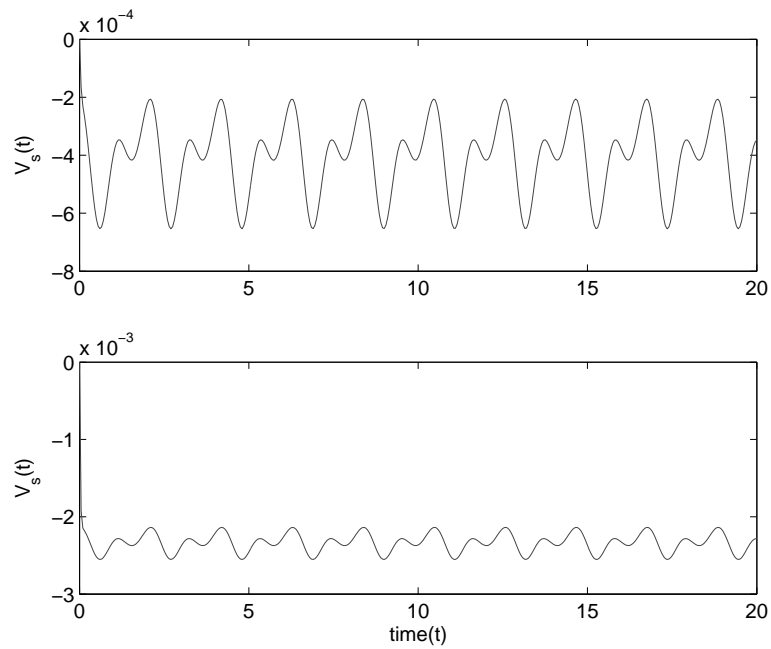
Figure 3: In this Figure, we demonstrate that the subthalamic interactions have no effect on the occurence of spike-wave like activity. The two graphics are numerical simulations of system (1) using XPP. The top graphic shows $V_s(t)$ with ν_{sr} non-zero. The bottom graphic shows the same system with $\nu_{sr} = 0$. In both cases the abnormal rhythm persists, with the subthalamic input acting effectively as an amplifier.
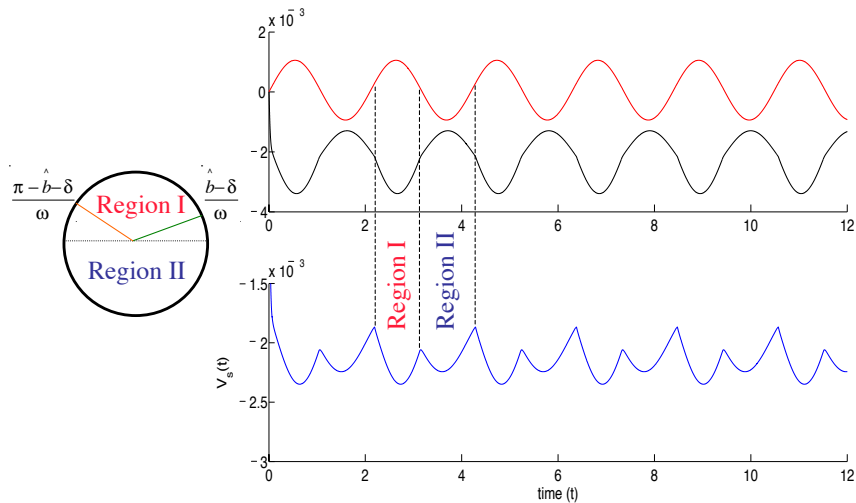
Figure 4: (COLOUR ONLINE) In the top graphic, the upper solution (in red) is the solution of the system when driven by the periodic forcing term $v_{se} \sin(\omega t)$ and the lower solution, is that of the system when driven by the composition of the piecewise linear approximation $y_\sigma(v)$, and $V_r(t)$. The difference in amplitudes of the second solution on each of the regions, combined with Region I being less than half the period gives rise to the spike-wave activity, illustrated in the lower graphic. The length of these regions can be adjusted by varying the parameters $\hat{b} = \arcsin\left(\frac{b}{K}\right)$ and δ as indicated on the circle. Notice that the peaks of both functions are slightly different due to the different phaseshifts δ and $\widehat{\delta}$, but these are not a primary cause of the final form of the solution.
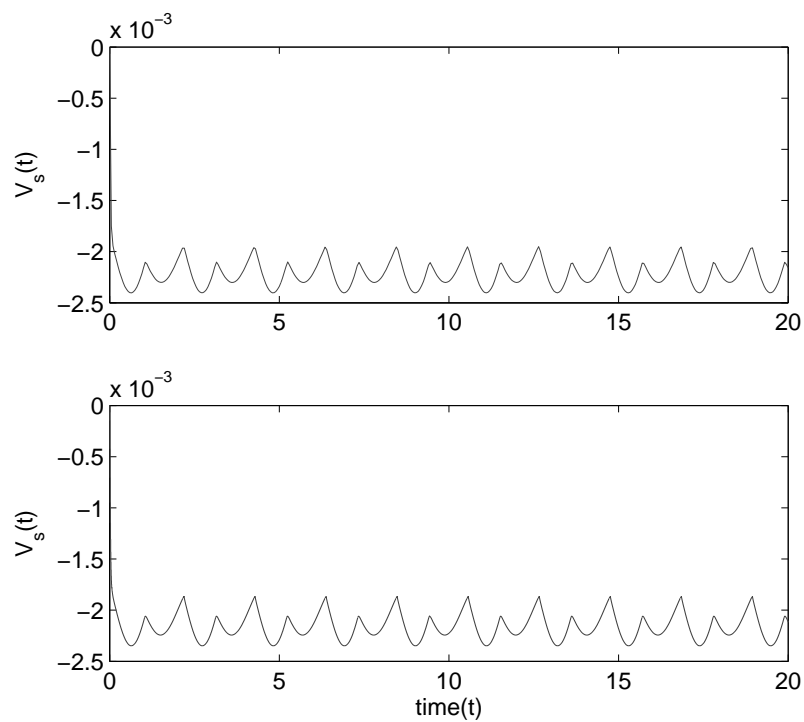
Figure 5: The top graphic shows the solution of $V_s(t)$ from the numerical package XPP for the peicewise linear system in the absence of v_{sn}. The bottom graphic shows the explicit solution obtained, demonstrating precise agreement between the numerics and our analysis.

Quantity	Description	*Petit Mal*
θ	Threshold of membrane potential before a cell fires.	0.015 V
σ	Standard deviation of neuron firing probability,versus cell membrane potential.	0.006 V
Q^{max}	Mean maximum firing rate of a cell.	250 s^{-1}
α	Receptor offset time constant (inverse of decay time of potential produced at synapse).	50 s^{-1}
β	Receptor onset time constant (inverse of inverse rise time of potential produced at synapse).	200 s^{-1}
ν_{sn}	Subthalamic signal strength.	20e-4 Vs
ν_{se}	Coupling strength between *external signal* and *specific relay* neurons.	44e-4 Vs
ν_{sr}	Coupling strength between *reticular* and *specific relay* neurons.	-8e-4 Vs
ν_{re}	Coupling strength between *external signal* and *relay nuclei*.	$16e-4$ Vs
ν_{rs}	Coupling strength between *specific relay* and *reticular* neurons.	6e-4 Vs

Table 1: Typical parameter values for the model to replicate *spike-wave* dynamics.